Application of Neural Networks to the Simulation of the Heat Island over Athens, Greece, Using Synoptic Types as a Predictor

GIOULI MIHALAKAKOU, HELENA A. FLOCAS, MANTHAIOS SANTAMOURIS, AND COSTAS G. HELMIS

Department of Physics, Division of Applied Physics, University of Athens, Athens, Greece

(Manuscript received 1 June 2001, in final form 6 December 2001)

ABSTRACT

The effect of the synoptic-scale atmospheric circulation on the urban heat island phenomenon over Athens, Greece, was investigated and quantified for a period of 2 yr, employing a neural network approach. A neural network model was appropriately designed and tested for the estimation of the heat island intensity at 23 stations during the examined period. The day-by-day synoptic-scale atmospheric circulation in the lower troposphere for the same period was classified into eight statistically distinct categories. The neural network model employed as an input the corresponding synoptic categories in conjunction with four meteorological parameters that are closely related to the urban heat island. It was found that the synoptic-scale circulation is a predominant input parameter, affecting considerably the heat island intensity. Also, it was demonstrated that the high pressure ridge mostly favors the heat island phenomenon and categories characterized by intense northerly component winds are responsible for its nonappearance or termination.

1. Introduction

The urban heat island (UHI) phenomenon is mainly caused by the differences in the thermal structure between urban and rural environments that are associated with thermal properties of urban materials, urban geometry, air pollution, and the anthropogenic heat released by urban activities (Park 1986). The phenomenon may occur during day or nighttime periods, and its spatial and temporal pattern is strongly controlled by the unique characteristics of each urban area (Lyall 1977; Barring et al. 1985; Escourrou 1991; Eliasson 1996; Shahgedanova et al. 1997; Montavez et al. 2000). The heat island intensity can be quantified by the maximum difference between urban temperature and the background rural one and depends on the size, population, and industrial development of the city, topography, physical layout, regional climate, and meteorological conditions (Oke et al. 1991).

The effect of meteorological parameters on UHI magnitude was the subject of considerable research (e.g., Johnson et al. 1991; Moreno-Garcia 1994; Kidder and Essenwanger 1995; Figuerola and Mazzeo 1998; Montavez et al. 2000; Morris et al. 2001). These studies revealed that wind speed and cloud amount are the most important parameters that influence the development and intensity of the UHI, suggesting that UHI intensifies under cloudless sky and light wind conditions.

However, only a few studies have addressed in depth the effect of the prevailing synoptic-scale weather conditions on the UHI phenomenon (Yague et al. 1991; Unger 1996; Morris and Simmonds 2000). More specific, Yague et al. (1991) and Unger (1996) employed a priori synoptic classification schemes of the surface synoptic-scale circulation in order to examine the variation of the UHI magnitude among the different synoptic categories (circulation to environment approach). On the contrary, Morris and Simmonds (2000) classified the UHI phenomenon according to its intensity and then examined the synoptic-scale circulation associated with each category (environment to circulation approach). Despite the approach and the classification scheme employed, these studies verified for different cities around the world that the UHI effect is stronger under anticyclonic conditions. Unlike the two former studies, Morris and Simmonds (2000) demonstrated that the lowest UHI magnitude does not occur under cyclonic conditions but rather during a northwesterly flow regime resulting from anticyclonic circulation.

The city of Athens is characterized by a strong heat island effect, mainly caused by accelerated industrialization and urbanization during recent years (Santamouris et al. 2001). The effect appears during both summer and winter periods, with mean daily intensity ranging between 6° and 12°C for the major central area (Santamouris et al. 1999a; Livada et al. 2001).

Neural networks are computational systems that sim-

Corresponding author address: Dr. H. A. Flocas, Department of Physics, Division of Applied Physics, University of Athens, Building PHYS-5, University Campus, GR-157 84 Athens, Greece.
E-mail: efloca@cc.uoa.gr

ulate, in a simple way, the structure and functions of the human brain (Li et al. 1990) and, therefore, are considered capable to model complex nonlinear processes. They belong to the class of ''data-driven'' approaches instead of ''model-driven'' methods because the analysis and the results depend on the available data (Chakraborty et al. 1992). Relationships between variables, models, laws, and predictions are constructed after building a machine that simulates the considered data. The process of constructing such a machine based on available data is addressed by using algorithms such as a perceptron or backpropagation (Rumelhart et al. 1986). Various researchers proposed neural algorithms for climatic and air quality time series predictions as well as for several energy applications (Hondou and Sawada 1994; Dash et al. 1995; Kalogirou et al. 1997; Mihalakakou et al. 1998; Santamouris et al. 1999b; Narasimhan et al. 2000). Especially for the study of the heat island phenomenon, Santamouris et al. (1999a) previously applied a neural network method for modeling the temperature distribution at various locations during the summer period in the greater Athens region.

The present paper aims at investigating the influence of the synoptic-scale circulation in the lower troposphere on the UHI over the greater Athens area (GAA) on a daily basis, utilizing a neural network approach. This approach allows the quantification of the relationship between synoptic-scale circulation and UHI magnitude as well as the assessment of the UHI under different synoptic conditions. The neural network system was designed and tested for estimating the urban heat island intensity in a considerable number of locations in the GAA, using as input the synoptic-scale circulation categories in conjunction with meteorological parameters that are strongly related to the heat island phenomenon.

2. The urban heat island experiment in Athens

The GAA is situated on a small peninsula located in the southeastern edge of the Greek mainland (Fig. 1). The central part of GAA is the Athens basin that covers an area of 450 km^2, with a population density of 8000 inhabitants per square kilometer. It is surrounded by mountains to the north (Parnitha, 1426 m), to the west (Egaleo, 458 m), and to the east (Hymettus, 1026 m, and Penteli, 1107 m) while it is open to the sea to the south (Saronicos Gulf). The other two parts of the GAA are the Thriassion Plain to the west of the Athens basin and the Mesogia Plain to the east. The small openings between the above-mentioned mountains play an important role in airmass exchange between the Athens basin and the Thriassion and Mesogia Plains (Helmis et al. 1997).

The urban heat island phenomenon over the GAA was examined using hourly measurements of ambient air temperature and humidity from 23 experimental stations, installed in the Athens urban and suburban regions (Fig. 1), for a period of 2 years, 1997–98. The sites were selected as a way to study areas with different building density and traffic load that are located along the north–south and east–west axes of the Athens basin and to get information about the boundary conditions around the basin.

A brief description of each experimental station is presented in Table 1. Seven stations were placed in the central area of Athens, and 15 stations were placed in urban areas and in a radial configuration around the center of Athens (see Fig. 1). Station 2 was situated in the slope of Hymettus Mountain (at an altitude of about 500 m), in an almost rural, non-built-up region with moderate vegetation and no traffic. The location of the station was selected in a way such that the effect of the local flows is substantially reduced. Since this station was nearly free from urban climate modifying effects, it was used as the reference station in this study.

Miniature data loggers equipped with a thermistor were used for measuring the hourly values of ambient air temperature at each experimental site. Since the majority of the sites are situated in street canyons, the most appropriate position for the installation of the instruments was the terrace of the first floor of high buildings or the top of low buildings, at a height of approximately 5 m. Consequently, for the remaining stations the instruments were installed at the same height in order to achieve similar conditions for all experimental results. A south orientation was selected for all instruments. The temperature sensors were calibrated and intercompared (accuracy of the sensors: ± 0.2°C). The storage capacity of the data loggers allows operation for approximately 300 days, with a resolution of 0.5°C.

The climate of GAA is typical ''Mediterranean,'' with a mild winter and dry hot summer. The monthly mean temperature varies between 9.3°C in January and 27°C in July, and the annual average precipitation is 376 mm. Prolonged sunshine duration is characteristic of the regional climate, with an annual value of 2884 h. At the synoptic scale, anticyclonic circulation prevails over the GAA in the lower troposphere throughout the year with maximum occurrence in January and June, and situations of cyclonic type dominate in February and March (Kassomenos et al. 1998a). A significant meteorological feature of the area is the high frequency of strong northeasterlies (well known as ''Etesians'') during summer, especially during July and August.

The synoptic-scale circulation in the lower troposphere over the examined area was typified at the isobaric level of 850 hPa rather than the surface in order to avoid topographic effects. The charts used for the day-by-day classification were drawn from the *European Meteorological Bulletin* archive for the period 1997–98. Data for 1200 UTC only were used for the study.

3. The neural network architecture

The estimation or prediction problem using neural network models can be separated into three steps or

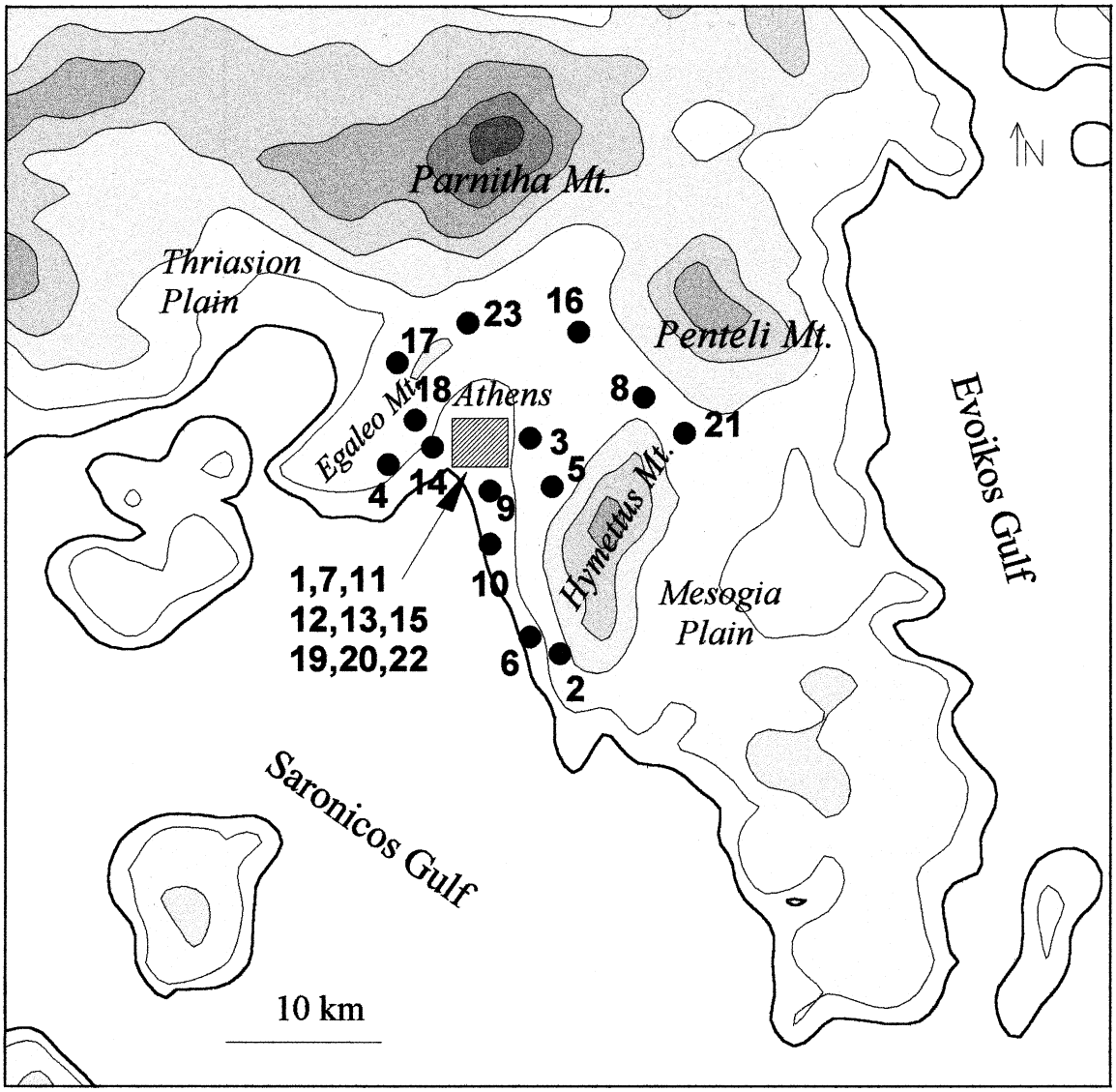

FIG. 1. Topography of the greater Athens area, where the locations of the 23 stations are displayed. Contours are every 200 m.

subproblems: designing the neural network architecture, conducting the learning or training process, and testing or diagnostic checking.

In this study a multilayered neural network architecture, based on the backpropagation algorithm, was selected for the estimation of the urban heat island intensity at each experimental site. Thus, a neural model was built separately for each of the 23 locations. The neural network model architecture consisted of one hidden layer of 20–25 so-called log-sigmoid neurons, followed by an output layer of one linear neuron. Learning was achieved using the backpropagation algorithm of Rumelhart et al. (1986) to train the network. An error goal of 0.5 was selected, and the number of epochs varied between 2000 and 3000. The main source of error seems to be the site-specific topographic conditions of some stations that cannot be perfectly described by the input parameters.

The input parameters of the neural models are as follows.

a. Synoptic-scale atmospheric circulation

The 850-hPa atmospheric circulation was classified into eight a priori categories on a daily basis for a 2-yr period (1997–98), for all seasons, according to the form and relative position of the synoptic-scale features typically representing the complete range of the atmospheric circulation over the Mediterranean basin. The occurrence of the heat island phenomenon is then assessed relative to the synoptic categories (circulation-to-environment approach).

TABLE 1. Characteristics of the experimental stations.

Station No.	Station characteristics
1	Central area. Low building density and absence of traffic.
2	Southeastern area. Rural, in the slope of Hymettus Mountain. No buildings, no traffic. Moderate vegetation.
3	Eastern area. Densely populated with much traffic.
4	Southwestern area. Less populated with low traffic, and negligible vegetation.
5	Eastern area. Highly populated with much traffic.
6	South coastal area, very close to the airport. Low traffic and very few buildings
7	Central area. Densely populated with heavy traffic.
8	Northeastern area. Increased building density and heavy traffic.
9	Southern area in a big avenue. Highly populated with heavy traffic.
10	Southern area, very close to the sea. Low building density and heavy traffic.
11	Central area in a pedestrian road. Very densely built and populated.
12	Central area. Increased traffic and very dense population.
13	Central area. High traffic and building density.
14	Central-western area in a university campus. Moderate vegetation, high traffic and low building density.
15	Central area. Densely populated with much traffic.
16	Northern area. Traffic is very low and trees are scattered all over the area.
17	Northwestern area at the edge of a planted area. Low traffic and building density.
18	Western area of Athens. Heavy traffic and high building density.
19	Central area. National park.
20	Central area. Archaeological place. Bare soil. No buildings. Some trees.
21	Northeastern suburban area. Increased traffic and average vegetation.
22	Central area. Heavy traffic. Large green spaces, consisting of gardens and trees.
23	North-central area in a big avenue. Not very densely built. High traffic.

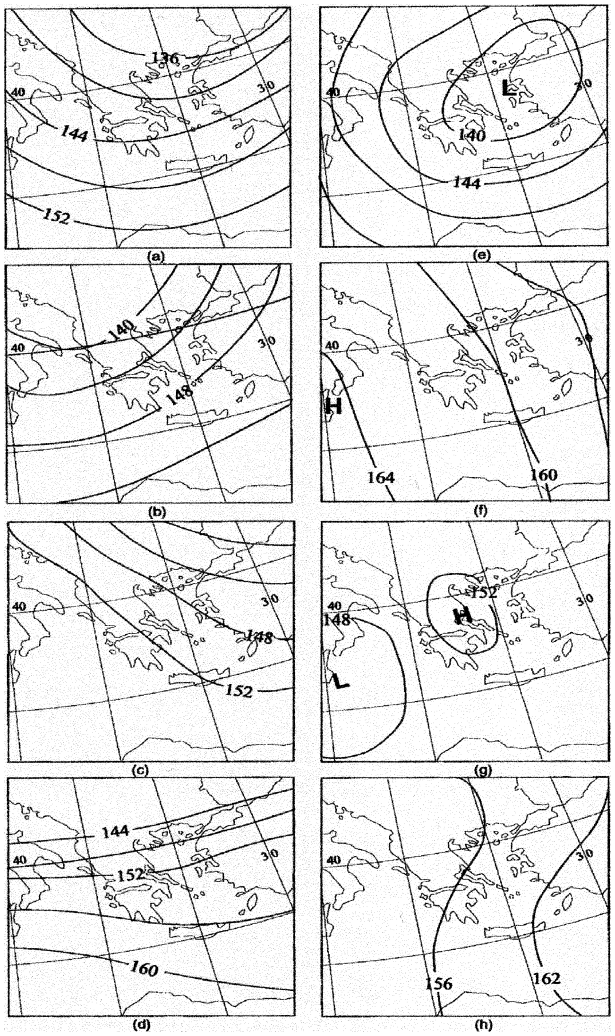

FIG. 2. Schematic presentation of the eight synoptic categories over GAA. See text for category descriptions illustrated in (a)–(g).

This manual classification scheme was proposed and employed by Kassomenos et al. (1998a) for the GAA for a period of 16 years (1980–95). According to this study, the employed synoptic categories proved to be statistically distinct at 850 hPa, with the aid of discriminant analysis. Using independent meteorological parameters from radiosonde data, a stepwise selection procedure based on Wilks's lambda criterion resulted in five parameters that discriminate the categories at 850 hPa. They are wind speed and direction, temperature, geopotential height, and equivalent potential temperature. The analysis demonstrated that a total of 80% of the objectively grouped cases correspond correctly to the a priori grouping for a randomly selected year. The synoptic categories, illustrated in Fig. 2, are as follows.

1) *Long-wave trough.* Greece is dominated by a long-wave trough with its axis being positioned over GAA (Fig. 2a). This category is characterized by intense winds, especially during the cold period of the year.
2) *Southwesterly flow.* A trough is observed southwest of the GAA, resulting in southwesterly flow, which is usually very strong. This category is accompanied by advection of warm and moist air masses from Africa (Fig. 2b).
3) *Northwesterly flow.* When the trough has passed, a strong northwesterly flow is established over GAA. This category is characterized by strong cold air advection from the north or northwest (Fig. 2c).
4) *Zonal flow.* The circulation is almost zonal over the GAA, resulting in a prevailing westerly flow (Fig. 2d) with considerably lower intensity in the warm period of the year.
5) *Closed low.* This category is characterized by the presence of a closed low, being accompanied by intense winds, usually from the northern sector, and rainfall (Fig. 2e).

6) *High pressure ridge.* A large-scale ridge dominates over the Greek area, usually for several days (Fig. 2f). This category is characterized by a very weak pressure gradient and weak, variable winds or calm conditions.
7) *Closed anticyclone.* This category is characterized by the presence of a closed anticyclone that extends over the major Greek area (Fig. 2g), being accompanied by weak winds from the southern or northern sector.
8) *Category high–low.* This category represents situations where a ridge is combined with a trough over the central-eastern Mediterranean basin, resulting in rather complicated regimes over GAA. In the warm period this category is mainly characterized by strengthening of the pressure gradient and strong northeasterlies (Etesians) that blow over the Aegean Sea and into the GAA (Fig. 2h).

The application of a proportional equality *t* test between the number of appearance days of each synoptic category during 1997 and 1998 and the corresponding number during the 16-yr period 1980–95 confirmed that the two years used in this study can be considered ''normal.''

b. Ambient air temperature measured at each station

This parameter is measured at each station when the maximum heat island intensity is observed. Usually, the air temperature in the urban environment is significantly higher than the corresponding rural temperature.

c. Ambient air temperature measured at the reference station

This input parameter is measured at the reference station when the maximum heat island intensity is observed. The reference temperature represents the energy balance at the reference station, which is regarded as representative of the surrounding countryside climatic conditions.

d. Maximum daily values of total solar radiation

Shortwave radiation is an important factor for the urban heat island estimation as it represents the amount of energy that arrives at the earth's surface as direct and diffused radiation. Urban surfaces have a significantly different behavior in comparison with the surrounding countryside ground surfaces with respect to absorption and reflectance. Roads and buildings absorb higher amounts of solar radiation whereas in the open countryside much incoming solar radiation is used for the evaporation of moisture. This is due to the geometry of urban areas that contributes to the trapping of shortwave radiation in the urban canyons. Moreover, urban albedo is significantly lower than the rural areas, thus contributing to a reduction of the reflected shortwave radiation. In our model, maximum daily values of total solar radiation were employed, being measured on a horizontal surface at the radiometric station of the National Observation of Athens (station 1).

e. Mean daily values of wind speed

Calm or low wind conditions are found to be conducive for strengthening of the urban heat island, while increases in the wind speed restrict the development of the phenomenon (Unger 1996; Morris et al. 2001). In this study, the wind speed was inserted in the model in the form of the mean daily values measured at station 1.

4. Results and discussion

a. Modeling the urban heat island intensity

Training was performed using the input parameter values for the estimation of the heat island intensity for 500 days of 1997 and 1998. The training results were compared with the measured ones for each station, and the comparison showed that the estimated heat island intensity values perform well with the measured ones for the whole set of experimental stations. Figure 3 shows the comparison between the estimated heat island intensity values using the neural model and the measured ones for six randomly selected stations. It can be seen that there is good agreement between estimated and measured values. The correlation coefficients fluctuated between 0.90 and 0.97 while the root-mean-square errors varied in the range of 0.1°–0.4°C.

Similar results were achieved for the whole set of the 22 stations. The correlation coefficients varied between 0.85 and 0.97, while the root-mean-square errors varied from 0.1° to 0.6°C. The urban stations, which are characterized by heavy traffic, increased air pollution, and building density, yield the better estimations. In these stations (numbers 3, 7, 9, 11, 12, 13, 15, 18, 20, 21, 23) the correlation coefficient has values between 0.90 and 0.97. For the remaining stations the correlation coefficient is slightly lower, varying from 0.83 to 0.92, since these stations are influenced by local flows, such as the sea breeze from the Saronicos Gulf (stations 6 and 10), katabatic and anabatic wind flows (stations 1, 5, and 8), or other site-specific factors, such as high vegetation (stations 14, 16, 19, and 22), and low traffic and building density (stations 4 and 17).

In order to test the results of the neural network, the model estimations were compared with the corresponding measurements of UHI intensity for the remaining 230 days of 1998 that compose the test dataset. Figure 4 presents the temporal variation of the estimated and measured UHI intensity values, for the testing set of measurements for 30 consecutive days of August 1998 and for four randomly selected stations. High values of the UHI intensity are achieved for all stations and es-

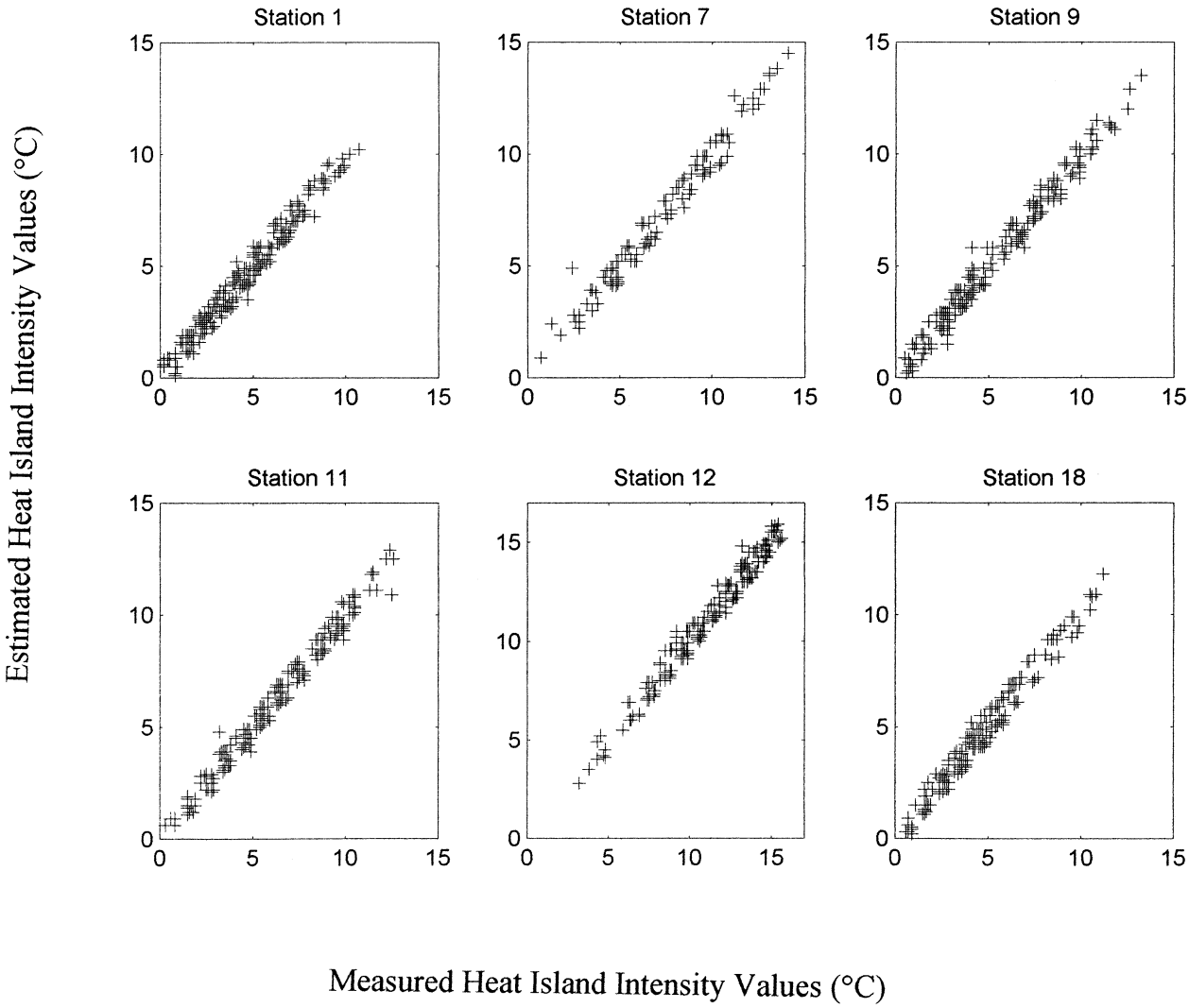

FIG. 3. Comparison of the measured and neural network–estimated urban heat island intensity values, for the training set of data and for six randomly selected experimental stations. The horizontal axis represents the measured values, and the vertical axis is the estimated values.

pecially for station 12, which is regarded as the most representative of strong urban conditions as it is characterized mainly by heavy traffic, increased air pollution, and high building density. Good agreement is observed between the estimated and measured data for the whole set of testing data: 90% of the relative error values range between −10% and 14%. The correlation coefficients between measured and estimated values vary from 0.86 to 0.94 while the root-mean-square errors range between 0.1° and 0.3°C.

b. Influence of synoptic circulation on the heat island intensity

The influence of each synoptic category was examined, based on the correlation coefficient between the measured and the estimated values of the UHI intensity. It was found that the synoptic category associated with the highest correlation coefficient (for 85% of the UHI days) is 6, implying that this category mainly favors the development of UHI phenomenon. This is because this category is characterized by a weak flow regime, while it is the most frequent during the warm period (May–September) as compared with the other categories. Its relative frequency of appearance during the examined period was 43%. The other anticyclonic category, 7, seems also to have an impact on the UHI phenomenon but considerably smaller, due to its very limited frequency of appearance (0.8%) during the warm period. It should be noted that the anticyclonic circulation mostly favors the development of the three sea breeze cells over GAA (Helmis et al. 1995, 1997), which acts to reduce the temperature in the southern and western suburbs of GAA during daytime, thus playing an important role in the evolution of the UHI event. Furthermore, Kassomenos et al. (1998b) have demonstrated that the

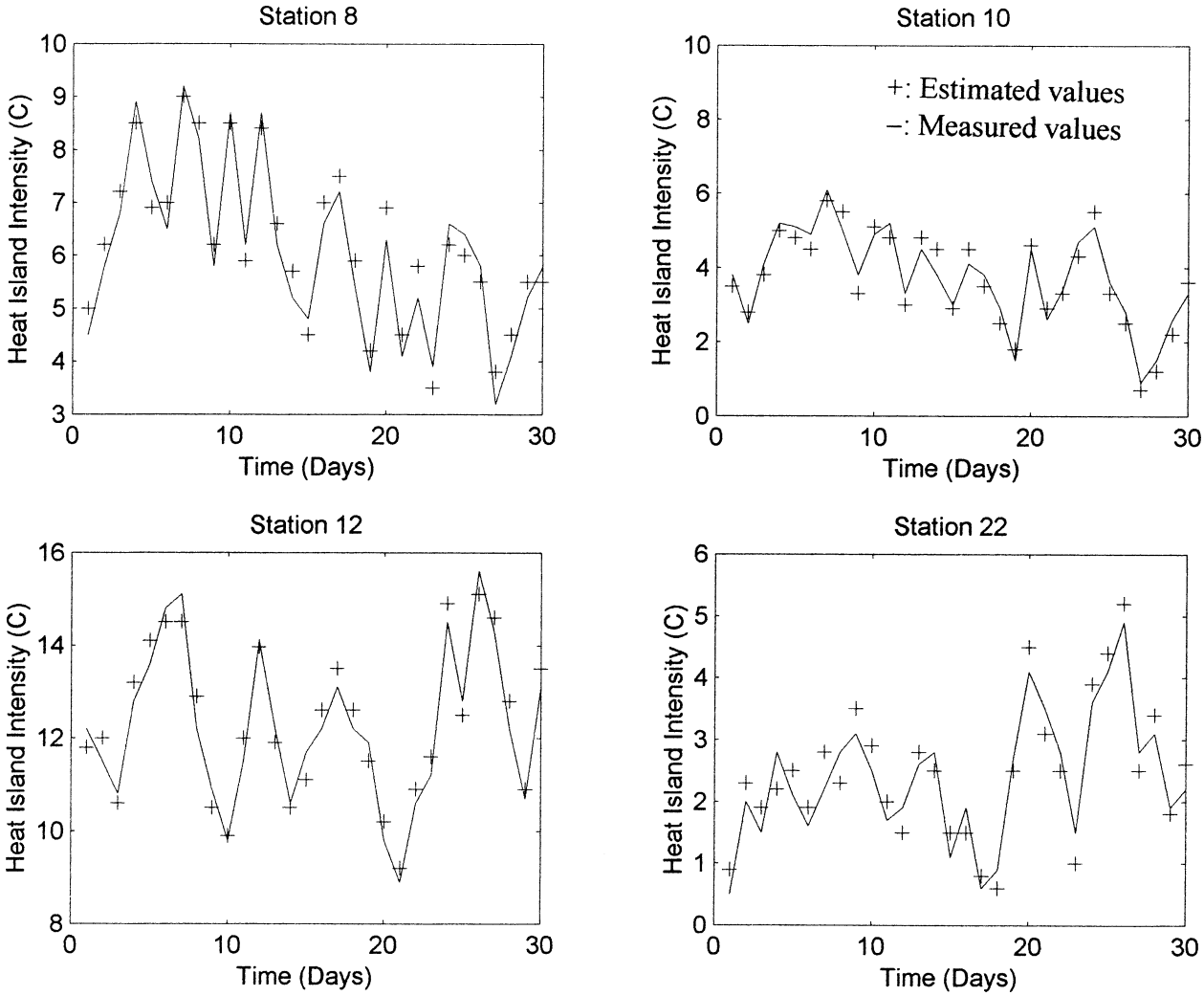

FIG. 4. Temporal variation of the estimated and measured urban heat island intensity values for 30 consecutive days of the testing period (1–30 Aug 1998) for randomly selected experimental stations.

anticyclonic patterns 6 and 7 during the warm period of the year are mostly connected to the formation of poor air quality conditions over the city center that further affect the UHI phenomenon. On the contrary, categories 3 and 8 do not improve significantly the correlation coefficient between the measured and simulated UHI intensity values and, therefore, seem to be responsible for the absence or termination of the phenomenon. This is attributed to the cold-air advection from the northwest that occurs over the GAA when category 3 prevails and the relatively colder air masses that are brought over GAA from the Aegean Sea because of the predominance of the category 8. Besides, these synoptic categories are found to be associated with the generation of strong mesoscale surface flows over GAA, which prevail during the warm period and especially in July and August (Kassomenos et al. 1998a).

In order to investigate the influence of atmospheric circulation on the estimation of the urban UHI intensity, neural network models were designed and trained using only the atmospheric circulation as input parameter, for 12 randomly selected experimental stations and for the same time period. Table 2 shows the correlation coefficients and the root-mean-square errors (rmse) between measured and estimated UHI intensity values when 1) all five previously presented parameters were used as inputs to the neural models (λ_1, rmse_1) and 2) atmospheric circulation was the only input parameter (λ_2, rmse_2). Moreover, Table 2 displays the percent reduction of the correlation coefficient λ_1 and λ_2. It was demonstrated that synoptic conditions as the only input parameter contributes significantly to the UHI intensity estimation with correlation coefficients as high as 0.77. The corresponding rmse ranges between 0.25 and 0.38 at the majority of the stations while higher values are realized at stations 6, 9, and 19. The correlation coefficient reduction between measured and estimated values varies between 18.1% and 26.4%. Therefore, it

TABLE 2. Correlation coefficients (λ) and root-mean-square errors (rmse) between the measured and neural network–estimated heat island intensity values when all parameters are used as inputs (λ_1, rmse_1), and when atmospheric circulation is the only input parameter, (λ_2, rmse_2).

Station No.	λ_1	λ_2	Rmse_1	Rmse_2	Reduction (%)
1	0.91	0.67	0.36	0.46	26.4
3	0.88	0.72	0.54	0.62	18.2
6	0.90	0.70	0.44	0.55	22.2
9	0.87	0.69	0.53	0.64	20.7
10	0.92	0.74	0.33	0.38	19.6
12	0.94	0.77	0.26	0.31	18.1
13	0.93	0.73	0.29	0.35	21.5
14	0.92	0.72	0.35	0.42	21.7
15	0.90	0.69	0.38	0.48	23.3
18	0.91	0.68	0.35	0.44	25.3
19	0.88	0.66	0.53	0.65	25.0
20	0.94	0.71	0.25	0.32	24.5

seems that atmospheric circulation affects considerably the UHI intensity, since it is responsible for the formation and evolution of the meteorological elements, which can enforce or eliminate the phenomenon. Similar results were also achieved for the whole set of the 23 stations.

5. Conclusions

The influence of the day-by-day synoptic-scale circulation in the lower troposphere on the urban UHI intensity over Athens was investigated, utilizing a neural network approach for a 2-yr period (1997–98). Five parameters were used as inputs to the model: synoptic-scale atmospheric circulation, ambient air temperature measured at each station, ambient air temperature at the reference station, maximum daily values of total solar radiation, and mean daily values of wind speed.

It was found that the estimated UHI intensity using the neural network model agrees well with the measured ones for both training and testing sets of measurements.

The neural network approach helped in quantifying the effect of the synoptic-scale circulation on the UHI intensity. The use of the synoptic-scale circulation as the only input parameter in the model resulted in high correlation coefficients between measured and estimated heat intensity values, reaching 0.77, and a reduction of the correlation coefficient of only 18.1%–26.4%, depending on the station, as compared with the case in which all five input parameters were incorporated. Therefore, it was found that the synoptic-scale circulation is a predominant input parameter, affecting considerably the UHI intensity.

Concerning the influence of each synoptic category on the UHI intensity, the neural network approach verified that anticyclonic categories 6 and 7 mostly favor the UHI over Athens, in agreement with previous studies that have employed different methodologies for other cities around the world. On the contrary, the northerly component airflow (categories 3 and 8) appears to limit the phenomenon.

REFERENCES

Barring, L., J. O. Mattsson, and S. Lindqvist, 1985: Canyon geometry, street temperatures and urban heat island in Malmo, Sweden. *Int. J. Climatol.,* **5,** 433–444.

Chakraborty, K., K. Mehrota, C. K. Mohan, and S. Ranka, 1992: Forecasting the behavior of multivariate time series using neural networks. *Neural Networks,* **5,** 961–970.

Dash, P. K., G. Ramakrishna, A. C. Liew, and S. Rahman, 1995: Fuzzy neural networks for time-series forecasting of electric load. *IEE Proc.—Gen. Transm. Distrib.,* **142,** 535–544.

Eliasson, I., 1996: Urban nocturnal temperatures, street geometry and land use. *Atmos. Environ.,* **30,** 379–392.

Escourrou, G., 1991: Climate and pollution in Paris. *Energy Build.,* **15–16,** 673–676.

Figuerola, P. I., and N. A. Mazzeo, 1998: Urban–rural temperature differences in Buenos Aires. *Int. J. Climatol.,* **18,** 1709–1723.

Helmis, C. G., K. H. Papadopoulos, J. Kalogiros, A. Soilemes, and D. N. Asimakopoulos, 1995: The influence of the background flow on the evolution of the Saronikos Gulf sea breeze. *Atmos. Environ.,* **29,** 3689–3701.

——, D. N. Asimakopoulos, K. H. Papadopoulos, P. Kassomenos, J. Kalogiros, and P. Papageorgas, 1997: Air mass exchange between Athens basin and Mesogia plain, Attica, Greece. *Atmos. Environ.,* **31,** 3833–3849.

Hondou, T., and Y. Sawada, 1994: Analysis of learning processes of chaotic time series by neural networks. *J. Prog. Theor. Phys.,* **91,** 397–402.

Johnson, G. T., T. R. Oke, T. J. Lyons, D. Steyn, I. D. Watson, and J. A. Voogt, 1991: Simulation of surface urban heat islands under ''ideal'' conditions at night—Part I: Theory and tests against field data. *Bound.-Layer Meteor.,* **56,** 275–294.

Kalogirou, S., C. Neocleous, S. Michaelides, and C. Schizas, 1997: A time series reconstruction of precipitation records using artificial neural networks. *Fifth European Congress on Intelligent Techniques and Soft Computing (EUFIT'97),* H. J. Zimmermann, Ed., Verlag Mainz, 2409–2413.

Kassomenos, P., H. A. Flocas, S. Lykoudis, and M. Petrakis, 1998a: Analysis of mesoscale patterns in relation to synoptic conditions over an urban Mediterranean basin. *Theor. Appl. Climatol.,* **59,** 215–229.

——, ——, A. N. Skouloudis, S. Lykoudis, V. Asimakopoulos, and M. Petrakis, 1998b: Relationship of air quality indicators and synoptic scale circulation at 850 hPa over Athens during 1983–1995. *Environ. Technol.,* **19,** 13–24.

Kidder, S. Q., and O. M. Essenwanger, 1995: The effect of clouds and wind on the difference in nocturnal cooling rates between urban and rural areas. *J. Appl. Meteor.,* **34,** 2440–2448.

Li, M., K. Mehrotra, C. K. Mohan, and S. Ranka, 1990: Sunspot numbers forecasting using neural networks. *Proc. IEEE Symp. Intelligent Control,* **1,** 524–529.

Livada, I., M. Santamouris, K. Niarchou, N. Papanikolaou, and G. Mihalakakou, 2001: Determination of places in the great Athens area where the heat island effect is observed. *Theor. Appl. Climatol.,* in press.

Lyall, I. T., 1977: The London heat island in June–July 1976. *Weather,* **32,** 296–302.

Mihalakakou, G., M. Santamouris, and D. N. Asimakopoulos, 1998: Modeling the ambient air temperature time series using neural networks. *J. Geophys. Res.,* **103,** 19 509–19 517.

Montavez, J. P., A. Rodriguez, and J. I. Jimenez, 2000: A study of the urban heat island of Granada. *Int. J. Climatol.,* **20,** 899–911.

Moreno-Garcia, M. C., 1994: Intensity and form of the urban heat island in Barcelona. *Int. J. Climatol.,* **14,** 705–710.

Morris, C. J. G., and I. Simmonds, 2000: Associations between varying magnitudes of the urban heat island and the synoptic cli-

matology in Melbourne, Australia. *Int. J. Climatol.,* **20,** 1931–1954.

——, ——, and N. Plummer, 2001: Quantification of the influences of wind and cloud on the nocturnal urban heat island of a large city. *J. Appl. Meteor.,* **40,** 169–182.

Narasimhan, R., J. Keller, and G. Subramaniam, 2000: Ozone modeling using neural networks. *J. Appl. Meteor.,* **39,** 291–296.

Oke, T. R., D. G. Johnson, D. G. Steyn, and I. D. Watson, 1991: Simulation of surface urban heat islands under 'ideal' conditions at night—Part 2: Diagnosis of causation. *Bound.-Layer Meteor.,* **56,** 339–358.

Park, H. S., 1986: Features of the heat island in Seoul and its surrounding cities. *Atmos. Environ.,* **20,** 1859–1866.

Rumelhart, D. E., G. E. Hinton, and R. J. Williams, 1986: Learning internal representations by error propagation. *Parallel Distributed Processing,* D. E. Rumelhart and J. L. McClelland, Eds., MIT Press, 318–362.

Santamouris, M., G. Mihalakakou, N. Papanikolaou, and D. N. Asimakopoulos, 1999a: A neural network approach for modeling the heat island phenomenon in urban areas during the summer period. *Geophys. Res. Lett.,* **26,** 337–340.

——, ——, B. Psiloglou, G. Eftaxias, and D. N. Asimakopoulos, 1999b: Modeling the global solar radiation on the earth surface using atmospheric, deterministic and intelligent data driven techniques. *J. Climate,* **12,** 3105–3116.

——, N. Papanikolaou, I. Livada, I. Koronakis, C. Georgakis, A. Argiriou, and D. N. Asimakopoulos, 2001: On the impact of urban climate on the energy consumption of buildings. *Sol. Energy,* **70,** 201–216.

Shahgedanova, M., T. P. Burt, and T. D. Davies, 1997: Some aspects of the three-dimensional heat island in Moscow. *Int. J. Climatol.,* **17,** 1451–1465.

Unger, J., 1996: Heat island intensity with different meteorological conditions in a medium-sized town: Szeged, Hungary. *Theor. Appl. Climatol.,* **54,** 147–151.

Yague, C., E. Zurita, and A. Marinez, 1991: Statistical analysis of the Madrid urban heat island. *Atmos. Environ.,* **25B,** 327–332.